Desalination and Water Treatment
www.deswater.com

doi:10.5004/dwt.2018.23259

135 (2018) 290–301
December

Enhancement of Reactive Red 198 dye photo catalytic degradation using physical mixtures of ZnO-graphene nanocomposite and TiO_2 nanoparticles: an optimized study by response surface methodology

Samer Abuzerr[a,b], Maher Darwish[c,d], Ali Mohammadi[c,e], Sara Sadat Hosseini[a], Amir Hossein Mahvi[a,f,*]

[a]*Department of Environmental Health Engineering, Faculty of Public Health, International Campus, Tehran University of Medical Sciences, Tehran, Iran, Tel. +98 90 34683920, email: samer_516@hotmail.com (S. Abuzerr), ssa_hosseiny@yahoo.com (S.S. Hosseini), Tel.+98 912 321 18 27, Fax +98 21 66744339, email: ahmahvi@yahoo.com (A.H. Mahvi)*
[b]*Quality Improvement and Infection Control, Ministry of Health, Gaza Strip, Palestine*
[c]*Pharmaceutical Quality Assurance Research Centre, Faculty of Pharmacy, International Campus, Tehran University of Medical Sciences, Tehran, Iran, Tel. +98.93.87563368, email: m-darwish@alumnus.tums.ac.ir (M. Darwish), Tel. +98.21.88358801, Fax +98.21.88358801, email: alimohammadi@tums.ac.ir (A. Mohammadi)*
[d]*Department of Pharmacy, Al-Safwa University College,Karbala, Iraq*
[e]*Nanotechnology Research Centre, Faculty of Pharmacy, Tehran University of Medical Sciences, Tehran, Iran*
[f]*Center for Solid Waste Research, Institute for Environmental Research, Tehran University of Medical Sciences, Tehran, Iran*

Received 20 January 2018; Accepted 6 October 2018

ABSTRACT

The photo catalytic activity of ZnO-graphene (ZnO-G) nanocomposite and TiO_2 nanoparticles physical mixtures for the enhanced degradation of reactive red dye 198 (RR198) under UVC light was evaluated and established. The photo catalytic results revealed that the RR198 was degraded at around 34.4% and 37.7% after 180 min of irradiation, respectively, in the presence of ZnO-G nanocomposite and TiO_2 nanoparticles, solely. Interestingly, physical mixtures of both catalysts induced an enhanced catalytic activity comparing to the bare ones. The ideal mixing ratio was found to be 66:34 wt% (ZnO-G:TiO_2) with 71.8% degradation performance after 180 min of irradiation. Moreover, the response surface methodology using the best mixture was employed to optimize and determine the interaction effects between three independent operational parameters which are photo catalyst dosage (0.4 – 0.025 mg), initial pH (3–11), and initial dye concentration (5 – 15 mg/L). Based on the results obtained, it was found that a maximum predicted degradation efficiency of RR 198 reached 99% was in agreement with the average of three experimental values (96%) under the following optimal conditions: 0.4 g mixture dose, initial pH of 3.8, and 5 mg/L initial dye concentration. This convergence between the predicted and experimental results indicates the validity of the model for predicting the maximum percentage degradation of RR198 under the above-mentioned optimum conditions. The ANOVA result indicated that the model is significant with the *P* value of 8.683×10^{-10} is less than 0.0001, which implies that the model terms are highly significant. Regression analysis with an R^2 value of 0.986 indicated a satisfactory correlation between the experimental data and predicted values. Additionally, non-toxic metabolites with respect to *Daphnia Magna* and high total organic carbon reduction after treatment with the mixture evidenced that this process can significantly decrease toxicity and mineralize the dye. Finally, the universal degradation ability of the photo catalysts mixture was evaluated and proven towards many model substrates.

Keywords: ZnO-graphene; TiO_2; Physical mixture; Photo catalytic degradation; Response surface methodology; Reactive red 198

*Corresponding author.

1. Introduction

Dyes are organic pollutants that are well known for their serious hazard on the whole ecosystem in general and aquatic life in particular. Textile, paper, tannery, and similar industries wastewater effluents contain a substantial amount of dyes. In order to reduce the negative effects of dye wastewater on humans and the environment, the wastewater must be treated efficiently before discharge into mainstreams [1,2]. It is worth mentioning that treatment of dye wastewater is highly complex due to the presence of color, toxicity, BOD, COD, turbidity, TDS, TSS, etc. However, various physical, chemical, and biological processes have been used over the past several decades for dyes treatment [3–9]. These techniques can, however, only transfer the contaminants from one phase to another, thus generating secondary pollution. In addition, conventional biological treatment methods are ineffective for decolorization and degradation because of the high stability of these dyes [10–12]. Consequently, traditional treatment methods are usually ineffectual in removing dyes. Hence, attention must be focused on treatment methods that can lead to the complete degradation of the dye molecules.

Recently, destructive processes such as advanced oxidation processes (AOPs) based on a semiconductor metal oxide photo catalyst have been effectively applied as an alternative for the decolorization and degradation of dyes in wastewater effluent [13,14]. During the AOP, a semiconductor material absorbs light of energy greater than or equal to its band gap, causing excitations of valence band electrons in the conduction band. Such charge separation leads to the formation of electron-hole pairs which can further generate free radicals in the system for redox of the substrate. The resulting free-radicals such as hydroxyl ($^{\bullet}OH$) are very efficient oxidizers of organic materials and can degrade pollutants [15–18]. Therefore, photo catalytic degradation using nanostructures is one of the most promising techniques to tackle the water contamination problem effectively in order to diminish the potential risks of such pollutants on human and the environment. The pros of such technologies include the use of environmentally friendly oxidants, complete mineralization of pollutants under mild temperature and pressure conditions, and the absence of waste disposal problem [19].

Among semiconductor metal oxides, TiO_2 and ZnO, are two of the most promising nano-crystalline materials used as photo catalysts in the degradation of organic pollutants due to their excellent photo catalytic activity,low cost, chemical stability, and non-toxicity [20–23]. However, the recombination of the photo excited electron-hole pairs, which in turn decreases the quantum yield and catalytic efficiency, is still a major hurdle of the applicability of such materials. Up to now, a variety of modifications have been proposed to overcome the limitations of TiO_2 by controlling the textural design, doping with metal or non-metal portions, and compositing with narrower band gap semiconductors and carbonaceous materials [24].

A considerable number of scientific reports have appeared on structuring TiO_2-ZnO, TiO_2-graphene, and ZnO-graphene nanocomposites for the efficient degradation of organic pollutants.

For instance, Topkaya et al. prepared b are ZnO and composite TiO_2-ZnO catalyst plates for the photo catalytic degradations of reactive red 180, pesticide (2,4-D), and enrofloxacin antibiotic under UVA and UVC irradiations. The plates were found to be more effective for the consecutive degradation tests which indicated their potentiality in extended applications [25]. Xie et al. prepared a series of TiO_2/ZnO composites with different content of TiO_2. Photo catalytic activity of the samples for the degradation of pentachlorophenol indicated that the optimal mole ratio of TiO_2 to ZnO was 0.75:1. However, they found that all the as-prepared TiO_2/ZnO composites not only had good catalytic activity under UV light irradiation but also have excellent circulation stability [26].

Liu et al. synthesized TiO_2–graphene nanocomposites are synthesized with tunable TiO_2 crystal facets ({100}, {101}, and {001} facets) through an anion-assisted method. TiO2-100-G showed the fastest charge-transfer rate, leading to higher activity in photo catalytic H_2 production from a methanol solution. TiO_2-101-G with more reductive electrons and medium inter facial charge-transfer rate also showed good H_2 evolution rate. Only TiO_2-001-G showed the lowest H_2 evolution rate [27].

Besides the importance of developing efficient photo catalysts structures, optimization of the catalytic reactions parameters is a crucial issue to be addressed in order to realize the desired feasibility. However, dealing only with one factor at a time while holding other parameters constant is unsatisfactory due to the multilateral effect of the parameters. Moreover, the process is time-consuming and the true optimum conditions are hard to predict [28]. This will indirectly increase the cost of the overall process [29]. This obstacle can be judiciously bypassed through the application of response surface methodology (RSM). RSM is a combination of the statistical and mathematical method for optimization study in a complicated process [30]. RSM gives a lot of information from a small number of experiments compared to conventional methods. In addition, this statistical design of experiments taking into account the interaction effects between the studied parameters and can determine the combination of levels in order to optimize the process more accurately [31,32]. A central composite design (CCD) based on RSM was successfully applied in the optimization of photo degradation of various organics [33,34].

To the best of our knowledge, the literature regarding the photo catalytic oxidation of RR198 using TiO_2 physically mixed with ZnO-G is not available yet. Therefore, a well-designed and parametric controlled heterogeneous photo catalysis system has been developed using a simple RSM in order to maximize reactive red 198 removals benefiting the ideal mixing ratio of both catalysts.

2. Experimental

2.1. Materials and reagents

All materials were in analytical grade and used without any further purification. The used mono azo Reactive Red 198 dye with 95% purity was purchased from Alvan Sabet Company, Hamedan, Iran. The TiO_2 P25 nanoparticles were obtained from Evonik Degussa GmbH, Germany, while the ZnO-graphene nanocomposite was prepared according to our previous report [21]. Hydrochloric acid (HCl) and sodium hydroxide (NaOH) were obtained from Merck, Germany.

2.2. Photo catalytic degradation studies

The photo catalytic studies were carried out in a photo reactor with a cylindrical Pyrex-glass cell of a 1.0 L capacity (Fig. 1). In a typical experiment, 0.1 g of the photo catalyst (bare or mixed) was suspended in 0.4 L of the RR 198 solution at pristine pH (~5.5) and stirred in the dark for 60 min to attain the adsorption equilibrium before irradiation. For this purpose, a preliminary study was conducted to determine the state of adsorption equilibrium, where the solution was stirred without illumination and samples were taken every 10 min, eventually, the equilibrium was achieved so that there was no difference in the readings between the 50th and 60th min. The photo catalytic reactions were initiated by the irradiation with a 10 W UV-C lamp with a maximum wavelength of 254 nm placed in a quartz lamp holder immersed in the photo reactor cell. The whole reactor was cooled with passing water current in the jacket between the outer wall of the reactor and the solution wall. The flowed water temperature was kept at 25°C in order to adjust the effect of daily fluctuations of water temperature on photo catalytic degradation rates. Water tank inside the laboratory was designated for that mission.

All reactants in the reaction cell were stirred using a magnetic stirrer to ensure the complete suspension of catalyst particles. At 30 min irradiation intervals, 4 mL of the suspension was taken out, centrifuged and then filtered with a 0.025 µm Nylon filter to remove the catalysts particles. The absorbance of RR198 was determined at λ_{max} = 520 nm using UV-Vis spectrophotometer (Perkin Elmer UV-Vis spectrophotometer). Subsequently, the degradation rate was calculated according to the following expression:

$$D\% = \left[\frac{(C_e - C)}{C_e}\right] \times 100 = \left[\frac{(A_e - A)}{A_e}\right] \quad (1)$$

where A_e and C_e are the absorbance and concentration of RR 198 at equilibrium, A and C are the same after a certain time of irradiation.

After electing the ZnO-G:TiO_2 weight ratio with the best catalytic activity, the influence of experimental parameters such as the concentration of the dye, catalyst amount, and the solution initial pH was explored and established.

Furthermore, the photo catalytic degradation kinetic has been considered with the Langmuir-Hinshelwood model (L-H). The reaction rate constant (k) was calculated using plots of $ln\ (C/C_e)$ versus illumination time according to the following formula:

$$Ln\left(\frac{C}{C_e}\right) = -kt \quad (2)$$

2.3. Experimental design

The optimal parameters of the experiment for desirable were determined according to the related literature [35,36]. RSM was used to optimize the three parameters, X1 (0.4–0.025 mg), X2 (3–11), and X3 (5–15 mg/L) which represent (photo catalyst dosage, initial pH, and initial dye concentration), respectively. The three parameters were selected as independent variables while the degradation percentage of RR198 was the output response variable. Other factors such as stirring rate, temperature, and light intensity were held constant.

Data analysis, experimental design, and regression modeling were achieved using the statistical software R (R Core Team). In order to check the accuracy of the fitted model, a series of statistical analysis such as the normal plot, the residual analysis, the main and interaction effects, the contour plot, and analysis of variance (ANOVA) were examined.

Table 1 shows the ranges and levels of independent variables. Central composite design (CCD) was chosen to investigate the combined effect of the three independent variables by 22 sets of experiments, including eight replications at the center points with rota table alpha. The coded value of the parameters was computed using the following equation:

$$X_i = \left(\frac{(X_0 - X_1)}{\Delta X}\right) \quad (3)$$

where X_i is a coded value of the independent variables, X_0, X_1 and ΔX are the uncoded values at the center point of the variables, respectively.

2.4. Acute toxicity test and TOC reduction

After treatment with ideal ZnO-G:TiO_2 mixture under optimum conditions, The acute toxicity tests with *Daph-*

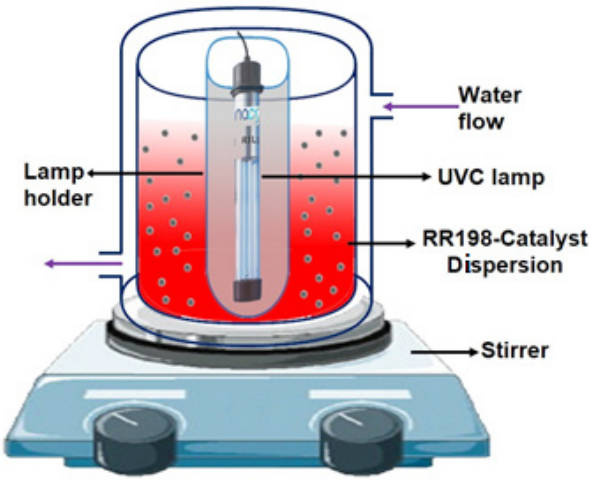

Fig. 1. Schematic diagram of the photo catalytic reactor system.

Table 1
Experimental range and levels of the independent variables for degradation of RR198

Variables	Symbols	Range				
		−α	–1	0	1	+α
Photo catalyst amount, g	X_1	0.1010	0.025	0.2125	0.4	0.3239
pH	X_2	4.6	3	7	11	9.4
RR198 concentration, mg/L	X_3	7	5	10	15	12.8

nia Magna were carried out according to the ABNT methodology as described by previous works [37,38]. The sensitivity tests were carried out with neonates (6–24 h of life), which were not fed during the test period. For each sample concentration, 10 organisms were used in a 5 mL flask in duplicates, along with the controls. The acute toxicity tests were conducted within 24–96 h of exposure and thereafter, the number of immobile organisms was observed and noted. The organisms were considered to be immobile if they did not show any mobility during 20 s of observation.

Also, as degradation might not be a veracious description of the photo catalytic process and the photo degradation might be a discolor process only, the change in organic carbon of the treated samples under the optimum conditions was monitored by measuring the total organic carbon (TOC) using a TOC analyzer type (TOC-V, Shimadzu).

3. Results and discussion

3.1. Influence of the photo catalyst composition

Obtaining the photo catalyst composition with the highest catalytic efficiency is the ultimate goal of our study. Hence, the catalytic performance of our samples (bare and mixed) was evaluated for the photo degradation of RR 198 under UVC light irradiation for 360 min in order to explore the correlation between the mixing ratio and photo degradation efficiency. The higher performance was taken as the decisive factor for selecting the sample that will be used for the experimental design study.

The normalized concentration changes of RR198 using the different photo catalysts under similar conditions are illustrated in Fig. 2. Looking at the dark phase, one can see an overall adsorption 25–45% for all samples which is considered a good adsorption under the conditions of our study (400 mL of 10 mg/L RR 198). The more ZnO-G existed, the more adsorption achieved, reasonably due to the fast conjugation between RR 198 and the aromatic regions of graphene by π-π stacking interactions added to the hydrogen bonding and/or electrostatic interactions of RR198 and photo catalysts surface. However, the removal efficiency has not followed the adsorption order in all cases. The maximum removal reached ~77% and ~82% with the samples (75:25) and (66:34), respectively.

As shown in Fig. 3, the degradation percentages allow the activity of the photo catalysts to be ranked as 66:34 > 75:25 > 20:80 > 25:75 > 34:66 > 80:20 > 50:50 > 0:100 > 100:0 for ZnO-G:TiO_2wt%. Obviously, all mixtures surpassed the bare samples in RR198 photo degradation ability emphasizing that the expected enhancement in catalytic activity compared to the individual photo catalysts has been fulfilled .The improved adsorbency and carriers recombination suppression are believed to have triggered the higher activities of mixtures. However, the absence of a specific pattern in Fig. 3 makes it very hard to give a correct description of the differences among the mixtures.

Fig. 4 shows the linear plots of $ln(C/C_0)$ apparent first-order rate constants k for the photo degradation of RR 198 with physical mixtures of ZnO-G and TiO_2 under UV light after 180 min of illumination. The slopes of the plots which represent the photo catalyst reaction rate constants were calculated and listed in Table 2. It can be seen from this table that the reaction rate of 66:34 physical mixture was relatively high and almost three folds of the bare photo catalysts.

Based on the obtained results, 66:34 wt% ratio for ZnO-G:TiO_2 was considered for the further studies. The intersection of the two curves (C/C_0 and $1–C/C_0$) shows the half-life of RR198, which is the time needed for the concentration of RR198 to decrease by half. From Fig. 5 it can be seen that the concentrations of RR 198 diminished gradually as the exposure time increased. The bare ZnO-G and TiO_2 have shown approximate profiles whereas concentration decrease was more pronounced in the mixture case. Furthermore, the half-life value of RR 198 dropped dramatically to 15 min for the mixture while it was 30 min for ZnO-G and 75 min for TiO_2.

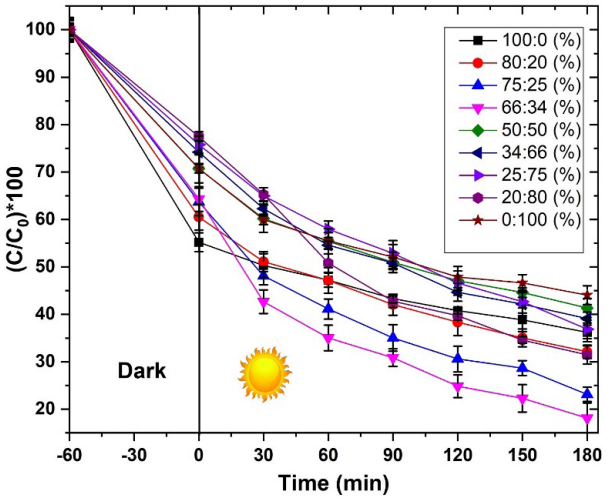

Fig. 2. Concentrations changes of RR198 in the presence of ZnO-G and TiO_2 nanoparticles with different mixing weight percentages under UV light.

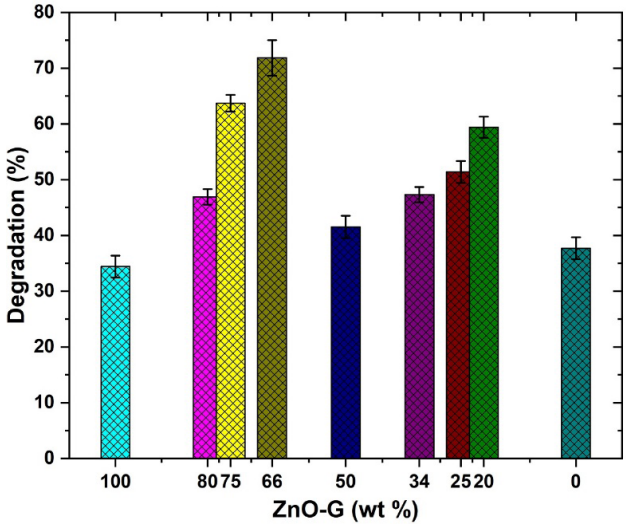

Fig. 3. Photo degradation of RR 198 over 180 min by excluding adsorption effect.

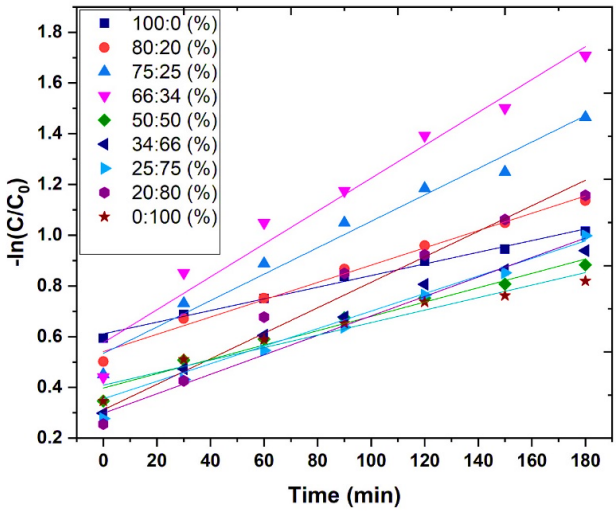

Fig. 4. The linear plots of $ln(C/C_0)$ for the photo degradation of RR 198 with physical mixtures of ZnO-G and TiO_2 under UV light after 180 min of illumination.

Table 2
Kinetic data of RR198 in the presence of ZnO-G and TiO_2 mixtures

ZnO-G:TiO_2 (wt%)	R^2	k
(100:0)	0.992	0.00230
(80:20)	0.989	0.00341
(75:25)	0.975	0.00521
(66:34)	0.966	0.00648
(50:50)	0.974	0.00282
(34:66)	0.973	0.00346
(25:75)	0.995	0.00384
(20:80)	0.970	0.00503
(0:100)	0.947	0.00246

3.2. Mechanism of photo catalytic activity

Prior proposing the mechanism of enhanced photo catalytic activity over ZnO-G:TiO_2 mixture, a transmission electron microscopy (TEM, 300 kV Philips CM30) was employed to observe the morphology of ZnO-G:TiO_2 (66:34). The obtained image (Fig. 6a) shows that in addition to the presence of graphene nanosheet-uniformly distributed hexagonal ZnO nanoparticles, few clusters of spherical shaped TiO_2 nanoparticles appeared. The TiO_2 clusters are observed inside the graphene nanosheets which ascertains an attachment to ZnO-G surface mostly via hydrogen bonding. Furthermore, the energy-dispersive spectrum (EDS, Mira 3-XMU Simaging Detectors) analysis confirmed the chemical composition of the product. The EDS spectra of ZnO-G:TiO_2 is shown in Fig. 6b. The mixture is free from elemental impurities and consists of Ti, Zn, O and C.

The presence of both C and O, as major elements, with strong Zn peaks implies that the graphene sheet is firmly coated with ZnO. The content of C, O, Zn, and Ti in the mixture is 16.37, 10.66, 55.14 and 17.46% weight, respectively.

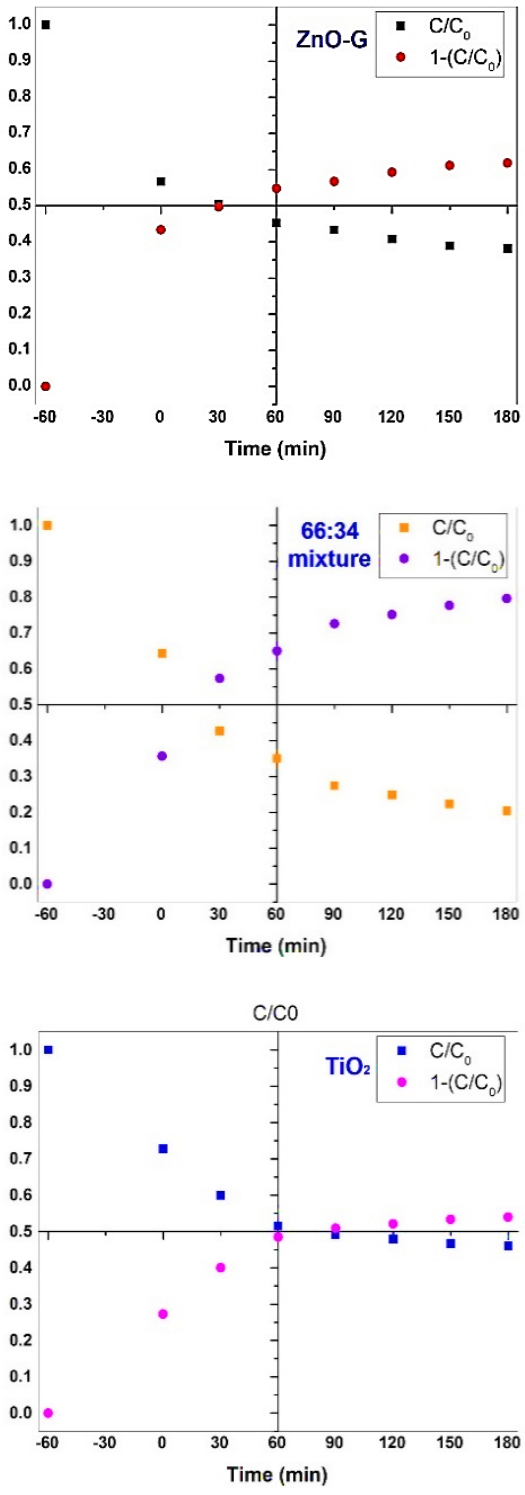

Fig. 5. Photo degradation profiles of RR198 by ZnO-G, TiO_2, and the ideal mixture.

Now that we have confirmed the composite-like structure of the physical mixture, control experiment to identify the contribution of reactive species was employing. In this experiment, isopropanol (IP) and benzoquinone (BQ) at (0.1×10^{-3} mol·L^{-1}) were used as scavengers for $HO^{\bullet}$ and $O_2^{-\bullet}$,

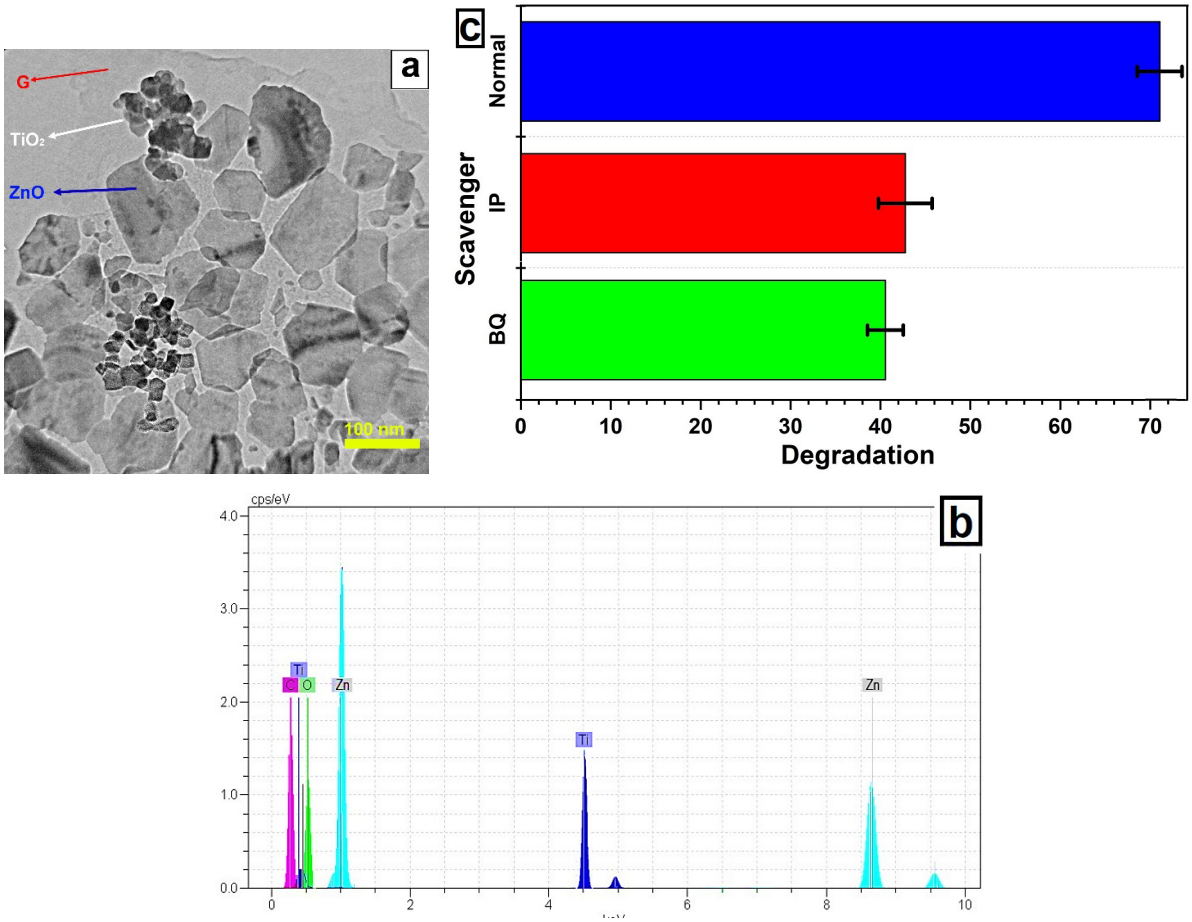

Fig. 6. TEM image (a) and EDS pattern (b) of the ideal ZnO-G:TiO_2 sample; Control experiment (c).

respectively. Degradation percentages depicted in Fig. 6c revealed that RR198 degradation was almost affected equally by quenching $HO^{\bullet}$ or $O_2^{-\bullet}$ which indicates an almost equivalent contribution of both $HO^{\bullet}$ and $O_2^{-\bullet}$ mediated mechanisms for RR 198 elimination.

The photo catalytic activity of ZnO-G and TiO_2 nanoparticles is strongly related to their band gap. TiO_2 has been reported with band gap energy of around 3.2 eV, while ZnO-G had an adsorption edge of around 371 nm corresponding to band gap energy of 3.3 eV. Although the band gap energies are similar to each other, nevertheless, the potential of the conduction band (CB) and the valence band (VB) of ZnO is charged a bit more negative. Post-irradiation, the mixture works as a heterostructure (Fig. 7) and the electrons are injected from the CB of ZnO to CB of TiO_2. These electrons in CB of TiO_2 can be subsequently transported to the graphene nanosheet that offers a high aptitude to accept and transfer the electrons. In addition, the holes are transferred from the VB of TiO_2 to VB of ZnO. As a result, recombination of the photo generated electron-hole charge carriers is markedly reduced. Then, the dissolved molecular oxygen reacts with electrons to yield super oxide radical anions. The holes are ultimately trapped by surface hydroxyl groups (or H_2O) on the surface of the photo catalyst to yield hydroxyl radicals. These reactive oxygen species contribute equally and efficiently to the redox reactions mediated decomposition of RR198.

3.3. Model fitting and statistically analysis

The response surface modeling based on experiments proposed by CCD with a total number of 22 experiments was applied in order to optimize the reaction conditions of RR 198 degradation. The experimental and predicted values under the various conditions are shown in Table 3.

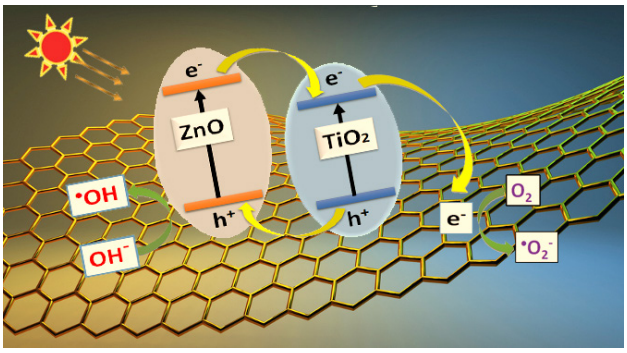

Fig. 7. Proposed charge transfer and the separation process on ZnO-G and TiO_2 mixture under UV-C.

Table 3
Central composite design with predictive values and their experimental results

	Independent variables			RR198 degradation (%)		
Run	X1 Photo catalyst amount (g)	X2 Initial PH	X3 Initial RR198 concentration (mg/L)	Experimental	Predictive	Residual
1	0.1010	9.4	13	44	41.962	–2.037
2	0.1010	4.6	13	64	62.292	–1.707
3	0.2125	7	10	53	53.581	0.581
4	0.3239	4.6	7	82	82.587	0.587
5	0.3239	9.4	13	65	66.002	1.002
6	0.1010	4.6	7	73	70.548	–2.452
7	0.3239	4.6	12.8	72	70.332	–1.668
8	0.1010	9.4	7	44	44.218	0.218
9	0.2125	7	10	56	53.581	–2.419
10	0.3239	9.4	7	72	72.257	0.257
11	0.2125	7	10	50	53.581	3.581
12	0.2125	7	10	54	53.581	–0.419
13	0.2125	7	5	61	61.126	0.126
14	0.2125	7	10	53	53.581	0.581
15	0.2125	11	10	74	73.634	–0.366
16	0.2125	7	10	54	53.581	–0.419
17	0.2125	7	15	47	48.924	1.924
18	0.2125	7	10	56	53.581	–2.419
19	0.025	7	10	30	32.856	2.856
20	0.2125	3	10	97	99.416	2.416
21	0.4	7	10	64	63.194	–0.8054
22	0.2125	7	10	53	53.581	0.581

On the other hand, ANOVA for response surface of triplet model was applied to evaluate the adequacy of the model. Table 4 shows the coefficient of the regression model and their significance while Table 5 shows the ANOVA for response surface of triplet model. In Table 5, the ANOVA indicated that the model is significant with the *P* value of 8.683×10^{-10} is less than 0.0001, which implies that the model terms are highly significant. Noteworthy, the values greater than 0.0001 designate that the model terms are not significant [39]. The non-significant "lack-of-fit value" of 0.205845 confirms the good predictability of the model [30]. Also, the "predicted R^2" of 0.986 is in reasonable agreement with the "adjusted R^2" of 0.976, which highlights the respectable predictability of the model [40]. The accuracy of the model is demonstrated in Fig. 8, which displays the experimental and predictive values for the degradation of RR 198. It clearly shows the high correlation between the experimental data and predicted values in the range studied.

Table 4
Coefficient of regression model and their significance

Factor	Coefficient estimate	Standard error	F Value	*P* Value	Explanation
Intercept	53.581	0.801	66.878	$<2.2 \times 10^{-16}$	Sig.
X1-catalyst amount	15.169	1.032	14.699	4.900×10^{-9}	Sig.
X2-pH	–12.891	1.032	–12.491	3.089×10^{-8}	Sig.
X3-initial concentration	–6.101	1.032	–5.912	7.119×10^{-5}	Sig.
X1:X2	11.314	2.268	4.989	0.0003151	Sig.
X1X3	–2.828	2.268	–1.247	0.2360978	Non-Sig.
X2:X3	4.242	2.268	1.971	0.0859378	.
$X1^2$	–5.556	1.629	–3.409	0.0051806	Sig.
$X2^2$	32.944	1.629	20.216	1.230×10^{-10}	Sig.
$X3^2$	1.444	1.629	0.886	0.3928765	Non-Sig.

Table 5
ANOVA for the response surface for RR198 degradation

Source	Degree of freedom	Sum of squares	Mean squares	F Value	*P* value	Suggestion
First-order response (x1, x2, x3)	3	2093.19	697.73	135.677	1.598×10^{-9}	Sig.
Two way interactions (x1, x2, x3)	3	154.00	51.33	9.982	0.001396	Sig.
Pure quadratic response (x1, x2, x3)	3	2186.91	728.97	141.752	1.238×10^{-9}	Sig.
Residuals	12	61.71	5.14	–	–	–
Lack of fit	5	35.84	7.17	1.939	0.209	Non-Sig.
Pure error	7	25.88	3.70	–	–	–
Multiple R-squared: 0.9863, Adjusted R-squared: 0.976, F-statistic: 95.8 on 9 and 12 DF, *p*-value: 8.68310^{-9}						

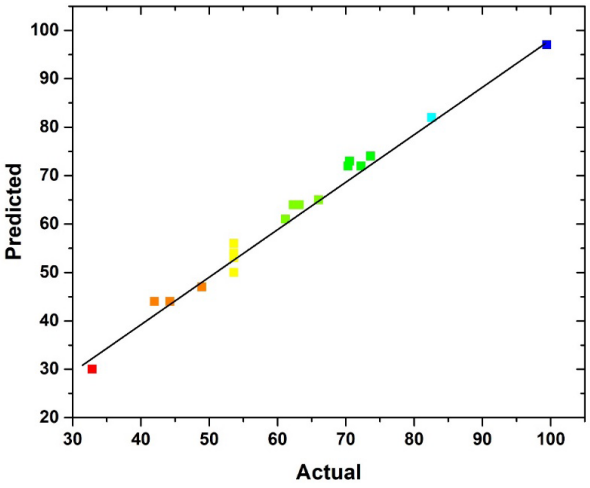

Fig. 8. Experimental values plotted against the predicted values for photo degradation of RR198.

An empirical second-order polynomial equation was realized and was written in terms of the independent factors based on Table 4 as follows:

$$D\% = 53.581 + 15.169(X1) - 12.891(X2) - 6.101(X3) + 11.313(X1X2) - 2.828(X1X3) + 4.242(X2X3) - 5.555(X1)^2 + 32.944(X2)^2 + 1.444(X3)^2 \quad (4)$$

The effect of the three independent variables and their second-orders except initial concentration was significant with $p<0.0001$. Based on the monomial coefficient values of regression model, P (X1-catalyst amount) = 4.900×10^{-9}, P (X2-pH) = 3.089×10^{-8}, and P (X3-initial concentration) = 7.119×10^{-5}, consequently the order of significance among the three independent variables was (X1-catalyst amount) > (X2-pH) > (X3-initial concentration). Similarly, the effect of the first order response [12], two-way interactions (TWI), and pure quadratic response (PQ) of (X1-catalyst amount, X2-pH, and X3-initial concentration) was significant with $p < 0.05$ since their P values were (1.598×10^{-9}, 0.001396, and 1.238×10^{-9}), respectively, which is attributed to the experimental range of independent variables chosen in this study. In addition, residuals analysis was conducted in order to check the suitability of the model. This was achieved by observing the normal probability plot of the residuals (Fig. 9a) where the residuals cloud narrowly distributed around a straight line proposing that the errors were distributed normally [41]. The other confirmation was by the plot of the residuals vs. the predicted response (Fig. 9b) where the

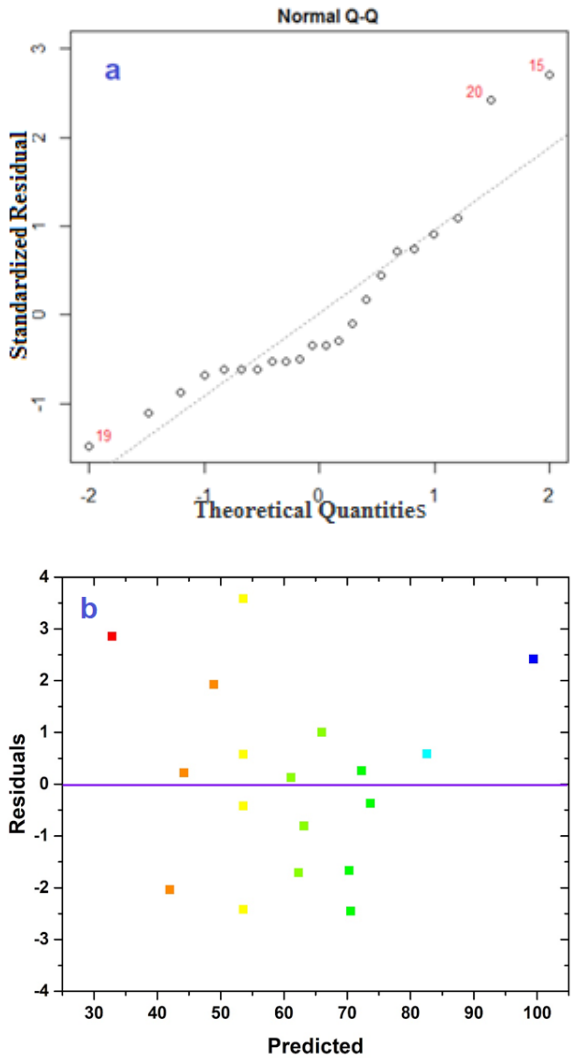

Fig. 9. Normal probability plots of the residuals (a) and plot of the residuals against the predicted response (b).

random pattern in the plot of residuals vs. the predicted response indicated the model is satisfactory and also the model does not interfere the independence or constant variance assumption [42].

3.4. Response surface analysis

Using of the three dimensions surface is popular to attain a clearer view of the interactions between variables within the range studied and can be provided as a graphical illustration of the regression equation adopted to determine the optimum values of variables [43]. The obtained results of the interactions between the three independent variables and the output response are depicted in Fig. 10. Fig. 10a displays that the high degradation efficiency is more obvious at lower levels of initial dye concentration and lower values of pH as observed in the contour plots. The RR 198 degradation efficiency had a maximum value at pH = 3. With increasing pH value to the neutral value, the degradation percentage collapsed to around 50%. Thereafter, at the basic medium showed a fair degradation but enhanced in comparison with the neutral medium. This can be attributed to the surface charge properties of the photo catalysts and ionization status of RR 198. The zero-point charge of TiO_2 and ZnO are at about (6.8 and 9, respectively) [44,45].

Below pH 6.8 a strong adsorption of dye on the photo catalyst surfaces as a result of the electrostatic attraction of the positively charged photo catalysts with the ionized dye. On the other hand, at neutral pHs, a decrease in the reaction rate has been observed reflecting the difficulty of an anionic dye in approaching the negatively charged ZnO-G surface due to electrostatic repulsion. At the basic medium, the degradation may be imputed to the abundant hydroxyl ions that would give a rise to the destructive hydroxyl radicals which in turn facilitate the dye decomposition.

Unsurprisingly, increasing the initial dye concentration induced a decrease in degradation performance. When the RR 198 concentration is increased, the production of hydroxyl radicals will slow down as fewer water molecules are adsorbed on the surface of the catalyst due to the competition by the excess dye molecules. Furthermore, increased pollutant concentration will hinder photon penetration into the solution and consequently, the photo degradation rate is decreased [46].

The effects of photo catalyst amount and the solution pH on RR198 degradation efficiency are shown in Fig. 10b. It is clear that the degradation efficiency markedly increases with increasing photo catalysts amount. This behavior can be related to the increased active sites on the surfaces of the abundant catalyst to harvest more photons which in turn increases the number of hydroxyl and super oxide radicals, and adsorb more pollutant molecules [47]. Thus, the overall activity is improved. Besides, degradation behavior as a function of pH replicated the results as in Fig. 10b, i.e. the preferred media can be ranged acidic > basic > neutral.

Fig. 10c depicts the influence of catalyst amount and initial RR198 concentration on the degradation efficiency while keeping pH at a pristine value (5.5). As presented on the surface, the degradation performance increased with increasing catalyst dosage in the studied range. Other than that, further enhancement in the dye concentration resulted in a lower percentage of degradation as interpreted above.

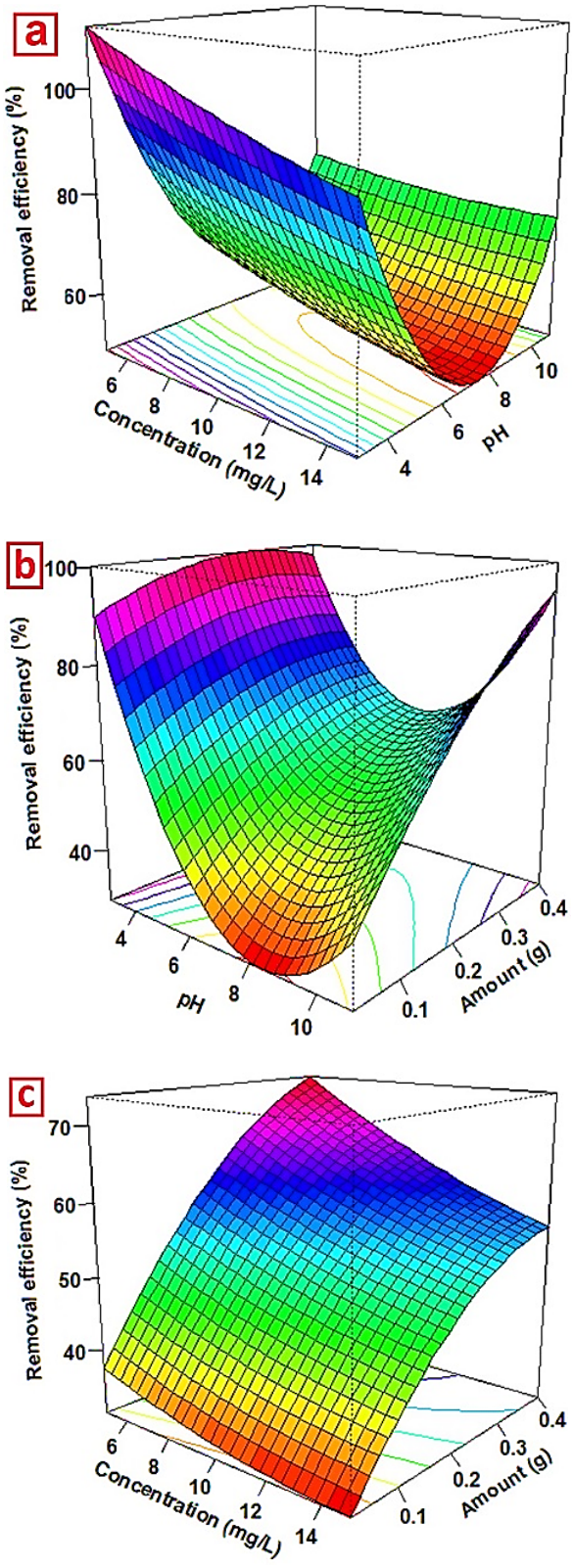

Fig. 10. Variables effect on the degradation efficiency of RR 198: (a) initial pH and initial dye concentration, catalyst amount was kept constant at 0.1 g; (b) catalyst amount and pH, initial dye concentration was kept constant at 10 mg/L; (c) catalyst amount and initial dye concentration, pH was kept constant at 5.5.

3.5. Optimization of the influencing variables

The goal of the optimization process is to achieve optimal conditions for degradation of R198 by the physical mixture of (64:34) ZnO-G nanocomposite: TiO_2 nanoparticles under UVC irradiation. RSM package in R software was utilized to determine the optimal values that maximize the intended functionality. The program uses five possibilities as a goal to construct desirability indices: none, maximum, minimum, target, and within range.

The criteria for all variables in correspondence with the predictive study are shown in Table 6. Under the optimum conditions for maximum RR198 degradation efficiency, pH value of 3.8, initial, dye concentration of 5 mg/L, and photo catalyst dosage of 0.4 g, a verification experiment was conducted for 180 min from three runs. The adequately approximate values between the predicted (99%) and the average experimental (96%) results demonstrate the validity of the model for predicting the maximum percentage degradation of RR 198.

3.6. Toxicity test and TOC reduction

The results for *Daphnia Magna* toxicity tests are expressed as the percentage of immobilization in the presence of treated samples (initial dye concentration of 5–15 mg/L) compared to the controls composed of the dye media without photo catalytic treatment. The controls displayed mortality between 33 to 41% at concentrations between 5–15 mg/L. 180 min photo degraded samples of all concentrations had almost no detectable toxicity suggesting that application of this process to detoxify RR180 significantly decreased the toxicity of solution. The TOC of the control medium (optimum conditions) was 1.72 mg/L. After decolorization for 180 min, around 62.8% of the initial TOC was abated (0.64 mg/L of TOC remained). This extent of TOC reduction demonstrates the high efficiency of the photo catalyst in degradation and further mineralization of RR 198.The Acute toxicity and TOC tests imply that the synergy between the catalytic compounds is not only demonstrated in terms of diminishing the amount of the RR 198 but also after decomposition more toxic compounds do not form and high extent of mineralization is obtained.

3.7. Universal activity of the mixture

In order to confirm the universal synergic degradation ability of the ideal mixture, photo catalytic activities were evaluated toward tetracycline (TC, the typical antibiotic), methylene blue (MB) and colorless phenol as typical organic compounds in water bodies. The degradation experiment of the three compounds was conducted by their solutions with a concentration of 10 mg/L under the same setup of RR198. The degradation behaviors against irradiation time are shown in Fig. 11.

We observed the degradation of around 98% of TC, 92% of MB and 92% of phenol molecules after 90 min, 120 min, and 180 min, respectively. At the same time, the removal yields of pure TiO_2 and ZnO-G were 58%, 53%, and 34% for TiO_2 and 66%, 78%, and 42% for ZnO-G toward TC, MB, and phenol, respectively. All the above proves that the ZnO-G:TiO_2 mixture enhances photo catalytic activity universally, which may represent a promising candidate for real application due to its high ability to decompose various contaminants in water.

Table 6
Optimum conditions for degradation of R198 and their predictive and experimental degradation percentages

Variable	Optimum value	Reactive Red 198 degradation (%)	
		Predictive	Experimental
(X1) Catalyst dosage *(g)*	0.4	99%	96%
(X2) initial pH	3.8		
(X3) initial dye concentration (mg/L)	5		

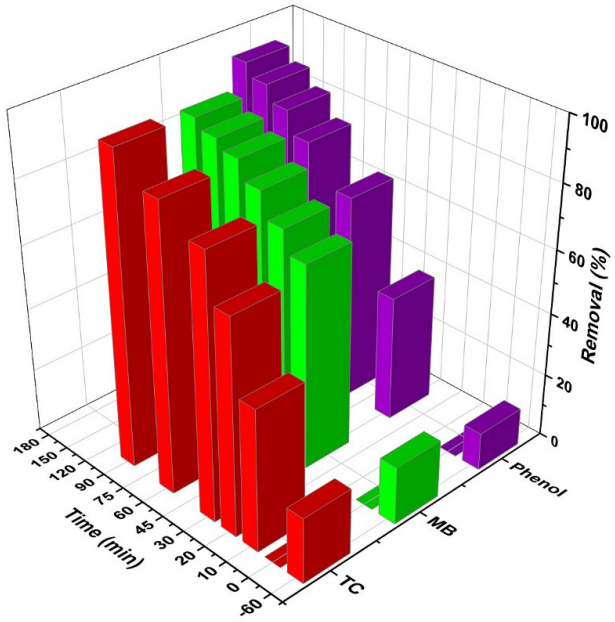

Fig. 11. The degradation behaviors against irradiation time for TC, MB, and phenol (10 mg/L) under the same other experimental conditions of RR198.

4. Conclusions

In this work, enhancement of reactive red dye 198 (RR198) photo degradation under UVC light established by following a simple physical mixture of ZnO-graphene (ZnO-G) nanocomposite and TiO2 nanoparticles. The results indicated that the RR198 was degraded at around 34.4% and 37.7% after 180 min of irradiation, respectively, in the presence of ZnO-G nanocomposite and TiO_2 nanoparticles, solely. Interestingly, physical mixtures of both catalysts induced an enhanced catalytic activity comparing to the bare ones. The ideal mixing ratio was found to be 66:34 wt% (ZnO-G:TiO_2) with 71.8% degradation performance. Moreover, a multivariate experimental design was applied

to develop a triplet model as the functional relationship between the three independent variables: the mixture dosage (0.4–0.025 mg), pH (3–11) and initial concentration of RR 198 (5–15 mg/L), to determine the optimum degradation percentage of RR198. The removal of RR 198 achieved 96% under optimal conditions: 0.4 g mixture dose, pH 3.8 and at 5 mg/L initial RR 198 concentration, which was in parallel with the maximum predicted degradation efficiency (99%). Regression analysis with an R^2 value of 0.986 indicated a satisfactory correlation between the experimental data and predicted values. Toxicity test with *Daphnia Magna* showed almost no toxicity of the by-products after the photo catalytic treatment. TOC reduction was 62.8% in the mixture stage demonstrating the high mineralization ability.

Acknowledgments

Authors would like to thank the laboratories team at Environmental Health Engineering Department, Tehran University of Medical Sciences, International campus for their materials and instrumental support. Also,we would like to express our gratitude for Eng. Shahrokh Nazmara, Eng. Hamidreza Ghaffari, Dr. Hoda Amiri, and Eng. Babak Mahmoudi for their technical assistance.

References

[1] S. Abuzerr, M. Darwish, A.H. Mahvi, simultaneous removal of cationic methylene blue and anionic reactive Red 198 dyes using magnetic activated carbon nanoparticles: equilibrium, and kinetics analysis, Water Sci. Technol., 2 2017 (2018) 534–545.

[2] M. Shirmardi, A. Mesdaghinia, A.H. Mahvi, S. Nasseri, R. Nabizadeh, Kinetics and equilibrium studies on adsorption of acid red 18 (Azo-Dye) using multi wall carbon nanotubes (MWCNTs) from aqueous solution, J. Chem., 9 (2012) 2371–2383.

[3] N. Mirzaei, H.R. Ghaffari, K. Sharafi, A. Velayati, G. Hoseindoost, S. Rezaei, A.H. Mahvi, A. Azari, K. Dindarloo, Modified natural zeolite using ammonium quaternary based material for Acid red 18 removal from aqueous solution, J. Environ. Chem. Eng., 5 (2017) 3151–3160.

[4] E. Bazrafshan, F.K. Mostafapour, A.R. Hosseini, A. Rakhsh Khorshid, A.H. Mahvi, Decolorisation of reactive red 120 dye by using single-walled carbon nanotubes in aqueous solutions, J. Chem., (2013) Article number 938374.

[5] A. Maleki, A.H. Mahvi, R. Ebrahimi, Y. Zandsalimi, Study of photochemical and sonochemical processes efficiency for degradation of dyes in aqueous solution, Korean J. Chem. Eng., 27 (2010) 1805–1810.

[6] A. Dalvand, R. Nabizadeh, M.R. Ganjali, M. Khoobi, S. Nazmara, A.H. Mahvi, Modeling of reactive blue 19 azo dye removal from colored textile wastewater using L-arginine-functionalized Fe_3O_4 nanoparticles: Optimization, re-usability, kinetic and equilibrium studies, J. Magn. Magn. Mater., 404 (2016) 179–189.

[7] M. Shirmardi, A.H. Mahvi, B. Hashemzadeh, A. Naeimabadi, G. Hassani, M.V. Niri, The adsorption of malachite green (MG) as a cationic dye onto functionalized multi walled carbon nanotubes, Korean J. Chem. Eng., 30 (2013) 1603–1608.

[8] S.S. Mirzadeh, S.M. Khezri, S. Rezaei, H. Forootanfar, A.H. Mahvi, M.H. Faramarzi, Decolorization of two synthetic dyes using the purified laccase of paraconiothyrium variabile immobilized on porous silica beads, J. Environ. Health Sci., 12 (2014) Article number 6.

[9] F.G. Borujeni, A.H. Mahvi, S. Nasseri, M.A. Faramarzi, R. Nabizadeh, M. Alimohammadi, Enzymatic treatment and detoxification of acid orange 7 from textile wastewater, Appl. Biochem. Biotechnol., 165 (2011) 1274–1284.

[10] J. Sun, X. Yan, K. Lv, S. Sun, K. Deng, D. Du, Photo catalytic degradation pathway for azo dye in $TiO_2/UV/O_3$ system: hydroxyl radical versus hole, J. Mol. Catal. A: Chem., 367 (2013) 31–37.

[11] S.D. Ashrafi, S. Rezaei, H. Forootanfar, A.H. Mahvi, M.A. Faramarzi, The enzymatic decolorization and detoxification of synthetic dyes by the laccase from a soil-isolated ascomycete, Paraconiothyrium variabile, Int. Biodeterior. Biodegrad., 85 (2013) 173–181.

[12] A. Saffar-Teluri, S. Bolouk, M.H. Amini, Synthesis of ZnO micro crystals and their photo catalytic ability in the degradation of textile azo dyes, Res. Chem. Intermed., 39 (2013) 3345–3353.

[13] D. Zhang, F. Zeng, Synthesis of an Ag–ZnO nanocomposite catalyst for visible light-assisted degradation of a textile dye in aqueous solution, Res. Chem. Intermed., 36 (2010) 1055–1063.

[14] M. Darwish, A. Mohammadi, N. Assi, Partially decomposed PVP as a surface modification of ZnO, CdO, ZnS and CdS nanostructures for enhanced stability and catalytic activity towards sulphamethoxazole degradation, Bull. Mater. Sci., 40 (2017) 513–522.

[15] K. Bezerra, W. Teixeira, S. Costa, E. Sriubas Jr, S. Costa, Textile effluent treatment dyed with reactive dye red Drimaren CL-5B by photochemistry degradation with H_2O_2/UV, Proc. 13th AUTEX World Textile Conference, Dresden, Germany, (2013).

[16] W.-C. Lin, C.-H. Chen, H.-Y. Tang, Y.-C. Hsiao, J.R. Pan, C.-C. Hu, C. Huang, Electrochemical photo catalytic degradation of dye solution with a TiO_2-coated stainless steel electrode prepared by electrophoretic deposition, Appl. Catal. B., 140 (2013) 32–41.

[17] B.P. Nenavathu, A.K. Rao, A. Goyal, A. Kapoor, R.K. Dutta, Synthesis, characterization and enhanced photo catalytic degradation efficiency of Se doped ZnO nanoparticles using trypan blue as a model dye, Appl. Catal. A., 459 (2013) 106–113.

[18] W. Yin, W. Wang, L. Zhou, S. Sun, L. Zhang, CTAB-assisted synthesis of monoclinic BiVO4 photo catalyst and its highly efficient degradation of organic dye under visible-light irradiation, J. Hazard. Mater., 173 (2010) 194–199.

[19] A. Eshaghi, M. Pakshir, R. Mozaffarinia, Photo induced properties of nanocrystalline TiO_2 sol-gel derived thin films, Bull. Mater. Sci., 33 (2010) 365–369.

[20] M. Darwish, A. Mohammadi, N. Assi, Q.S. Manuchehri, Y. Alahmad, S. Abuzerr, Shape-controlled ZnO nanocrystals synthesized via auto combustion method and enhancement of the visible light catalytic activity by decoration on graphene, J. Alloys Compd., 703 (2017) 396–406.

[21] A. Mahvi, M. Ghanbarian, S. Nasseri, A. Khairi, Mineralization and discoloration of textile wastewater by TiO_2 nanoparticles, Desalination, 239 (2009) 309–316.

[22] O. Solcova, L. Spacilova, Y. Maleterova, M. Morozova, M. Ezechias, Z. Kresinova, Photo catalytic water treatment on TiO_2 thin layers, Desal. Water Treat, 57 (2016) 11631–11638.

[23] M. Darwish, A. Mohammadi, N. Assi, Integration of nickel doping with loading on graphene for enhanced adsorptive and catalytic properties of CdS nanoparticles towards visible light degradation of some antibiotics, J. Hazard. Mater., 320 (2016) 304–314.

[24] E. Topkaya, M. Konyar, H.C. Yatmaz, K. Öztürk, Pure ZnO and composite ZnO/TiO_2 catalyst plates: a comparative study for the degradation of azo dye, pesticide and antibiotic in aqueous solutions, J. Colloid Interface Sci., 430 (2014) 6–11.

[25] J. Xie, Y. Hao, M. Li, Y. Lian, L. Bian, Preparation of TiO_2/ZnO composite catalysts and their photo catalytic activity for degradation of pentachlorophenol, World J. Eng., 14 (2017) 279–283.

[26] L. Liu, Z. Liu, A. Liu, X. Gu, C. Ge, F. Gao, L. Dong, Engineering the TiO_2–graphene interface to enhance photo catalytic H2 production, Chem. Sus. Chem., 7 (2014) 618–626.

[27] S. Giri, N. Das, G. Pradhan, Synthesis and characterization of magnetite nanoparticles using waste iron ore tailings for adsorptive removal of dyes from aqueous solution, Colloids Surf., A., 389 (2011) 43–49.

[28] M.A. Bezerra, R.E. Santelli, E.P. Oliveira, L.S. Villar, L.A. Escaleira, Response surface methodology (RSM) as a tool for optimization in analytical chemistry, Talanta, 76 (2008) 965–977.
[29] K.M. Carley, N.Y. Kamneva, J. Reminga, Response surface methodology, in, Carnegie-Mellon Univ Pittsburgh PA School of Computer Science, 2004.
[30] E. Yücel, N. Güler, Y. Yücel, Optimization of deposition conditions of CdS thin films using response surface methodology, J. Alloys Compd, 589 (2014) 207–212.
[31] A. Babaei, A. Mesdaghiniai, N.J. Haghighi, R. Nabizadeh, A. Mahvi, Modeling of nonylphenol degradation by photo nanocatalytic process via multivariate approach, J. Hazard. Mater., 185 (2011) 1273–1279.
[32] H. Yang, S. Zhou, H. Liu, W. Yan, L. Yang, B. Yi, Photo catalytic degradation of carbofuran in TiO_2 aqueous solution: Kinetics using design of experiments and mechanism by HPLC/MS/MS, J. Environ. Sci., 25 (2013) 1680–1686.
[33] S. Kaur, V. Singh, Visible light induced sono photo catalytic degradation of Reactive Red dye 198 using dye sensitized TiO_2, Ultrason. Sonochem., 14 (2007) 531–537.
[34] A. Khataee, M.B. Kasiri, Photo catalytic degradation of organic dyes in the presence of nanostructured titanium dioxide: influence of the chemical structure of dyes, J. Mol. Catal. A: Chem., 328 (2010) 8–26.
[35] A. Eshaghi, S. Hayeripour, A. Eshaghi, Photo catalytic decolorization of reactive red 198 dye by a TiO_2–activated carbon nano-composite derived from the sol–gel method, Res. Chem. Intermed., 42 (2016) 2461–2471.
[36] A.H. Mahvi, A. Maleki, M. Alimohamadi, A. Ghasri, Photo-oxidation of phenol in aqueous solution: Toxicity of intermediates,Korean J. Chem. Eng., 24 (2007) 79–82.
[37] F. Gholami-Borujeni, A.H. Mahvi, S. Naseri, M.A. Faramarzi, R. Nabizadeh, M. Alimohammadi, Application of immobilized horseradish peroxidase for removal and detoxification of azo dye from aqueous solution, Res. J. Chem. Environ., 15 (2011) 217–222.
[38] M. Zarei, A. Niaei, D. Salari, A. Khataee, Application of response surface methodology for optimization of peroxi-coagulation of textile dye solution using carbon nanotube–PTFE cathode, J. Hazard. Mater., 173 (2010) 544–551.
[39] S. Chowdhury, P.D. Saha, Scale-up of a dye adsorption process using chemically modified rice husk: optimization using response surface methodology, Desal. Water Treat., 37 (2012) 331–336.
[40] S. Chatterjee, A. Kumar, S. Basu, S. Dutta, Application of response surface methodology for methylene blue dye removal from aqueous solution using low cost adsorbent, Chem. Eng. J., 181 (2012) 289–299.
[41] B.K. Körbahti, M.A. Rauf, Determination of optimum operating conditions of carmine decoloration by UV/H_2O_2 using response surface methodology, J. Hazard. Mater., 161 (2009) 281–286.
[42] A. Franco, M. Neves, M.R. Carrott, M. Mendonça, M. Pereira, O. Monteiro, Photo catalytic decolorization of methylene blue in the presence of TiO_2/ZnS nanocomposites, J. Hazard. Mater., 161 (2009) 545–550.
[43] D. Vildozo, C. Ferronato, M. Sleiman, J.-M. Chovelon, Photo catalytic treatment of indoor air: Optimization of 2-propanol removal using a response surface methodology (RSM), Appl. Catal., B., 94 (2010) 303–310.
[44] S. Kaur, V. Singh, Visible light induced sono photo catalytic degradation of Reactive Red dye 198 using dye sensitized TiO_2, Ultrason. Sonochem., 14 (2007) 531–537.
[45] Q.S. Manuchehri, N. Assi, S. Pourmand, M. Darwish, A. Pakzad, Photo catalytic activity of ZnO nanoparticles prepared by a microwave method in ethylene glycol and polyethylene glycol media: A comparative study, in: J. Nano Res, Trans Tech Publ., 2016, pp. 53–64.
[46] S. Pardeshi, A. Patil, Solar photo catalytic degradation of resorcinol a model endocrine disrupter in water using zinc oxide, J. Hazard. Mater., 163 (2009) 403–409.
[47] L. Wei, C. Shifu, Z. Wei, Z. Sujuan, Titanium dioxide mediated photo catalytic degradation of methamidophos in aqueous phase, J. Hazard. Mater., 164 (2009) 154–160.